Supporting Information

Phase-switchable catalytic system design for the efficient and economical conversion of fructose to 5-hydroxymethylfurfural

Fangyuan Zhou [a], Tianyi Long [a], Yitong Wang [a], Hongke Zhang [a], Tiansheng Deng [c], Bin Yang [d], Can Yin [a], Ming Xia*[b], Wanbin Zhu*[a], Hongliang Wang*[a]

[a] Center of Biomass Engineering /College of Agronomy and Biotechnology, China Agricultural University, Beijing, 100193, PR China

[b] State Key Laboratory of Materials-Oriented Chemical Engineering, College of Chemical Engineering, Nanjing Tech University, Nanjing, 211816, PR China

[c] Institute of Coal Chemistry, Chinese Academy of Sciences, 27 South Taoyuan Road, Taiyuan 030001, PR China

[d] Bioproducts, Sciences, and Engineering Laboratory, Department of Biological Systems Engineering, Washington State University, Richland, WA 99354, USA

* Corresponding author. E-mail: Hlwang@cau.edu.cn (H. Wang), wanbin@cau.edu.cn (W. Zhu), mxia@njtech.edu.cn (M. Xia).

Materials and Methods

Chemicals

D-fructose (99%), D-glucose (99.5%), 5-hydroxymethylfurfural (99%), levulinic acid (LA, 99 %), formic acid (FA, 99.5%), betaine (98%), betaine hydrochloride (BHC, 99%), γ-valeroactone (GVL, 98%), tetrahydrofuran (THF, 99.5%), 2-methyltetrahydrofuran (2-MTHF, 99%), methyl isobuty ketone (MIBK, 99%), dimethyl carbonate (DMC, 98%), ethyl acetate (EA, 99.5%), dimethyl sulfoxide (DMSO) and acetonitrile (ACE) were all purchased from Aladdin (Shanghai, China). HCl (36–38%), and acetone were purchased from Sinopharm Group Chemical Reagent Co. Ltd (Shanghai, China). All chemicals utilized in this research were commercially available and were not purified further.

Dehydration of fructose to HMF

Aqueous BHC solutions were prepared by dissolving predetermined amounts of BHC in deionized water. The mixture was stirred in a 50 °C water bath until a clear, homogeneous solution was obtained (no residual solids). The solution was cooled to room temperature and stored in a volumetric flask to minimize water evaporation prior to use. Fructose dehydration reactions were conducted in 20 mL thick-walled pressure tubes (Synthware Corporation). In a typical run: D-fructose (5.0–60.0 wt%) was dissolved in 2 mL of 40 wt% BHC aqueous solution; 8 mL of acetone was then added, and the tube was sealed tightly. The mixture was heated in a constant-temperature oil bath (90–120 °C) for 5 min to 6 h under magnetic stirring. After reaction, the mixture was cooled to room temperature, diluted with water, and filtered for subsequent analysis.

Product analysis

Quantitative analysis of fructose and reaction products was performed using a Shimadzu LC-20A high-performance liquid chromatography (HPLC) system equipped with an Aminex HPX-87 column (Bio-Rad) maintained at 40 °C. The mobile phase consisted of 5 mM aqueous H_2SO_4 solution, delivered at a flow rate of 0.6 mL min^{-1}. Fructose, formic acid (FA), and levulinic acid (LA) were detected using a refractive index detector (RID-20A), while HMF was analyzed via a photodiode array (PDA) detector (SPD-M20A) at a wavelength of 210 nm. Calibration curves were constructed using external standards to quantify analyte concentrations. Fructose conversion, HMF yield, and HMF selectivity were calculated using equations (1)–(3) as follows:

$$\text{Feedstock conversion (mol\%)} = \frac{\text{moles of reacted feedstock}}{\text{moles of initial feedstock}} \times 100 \quad (1)$$

$$\text{HMF yield (mol\%)} = \frac{\text{moles of produced HMF}}{\text{moles of initial feedstock}} \times 100 \quad (2)$$

$$\text{HMF selectivity (mol\%)} = \frac{\text{HMF yield}}{\text{Feedstock conversion}} \times 100 \quad (3)$$

Kinetic experiments

Kinetic studies of fructose dehydration were conducted over a temperature range of 90–120 °C under optimized reaction conditions. The analysis was based on the following assumptions:

(1) The primary reaction pathway is fructose to HMF, with side reactions neglected;

(2) The main reaction is irreversible and follows pseudo-first-order kinetics;

(3) All by-products are categorized as degradation products (e.g., humins).

Under these assumptions, rate constants at different temperatures were calculated using the Weibull equation:

$$-ln\left(\frac{C_t}{C_0}\right) = kt$$

where k is the reaction rate constant (min^{-1}), t is the reaction time (min), C_0 is the initial fructose concentration (mol/mL) at t = 0 min, and C_t is the fructose concentration (mol/mL) at time t. The activation energy for the reaction was estimated using the Arrhenius equation:

$$ln(k) = -\frac{E_a}{RT} + lnA$$

where E_a, T, R and A represent the activation energy (kJ/mol), reaction temperature (K), gas constant (0.008314 $kJ \cdot mol^{-1} \cdot K^{-1}$), and preexponential factor (min^{-1}), respectively.

Molecular dynamics simulations

Molecular Dynamics (MD) simulations were performed using the GROMACS 2019 software package to investigate the solvation behavior of fructose and HMF in the aqueous BHC/acetone reaction phase. Simulation systems were constructed as follows: 300 fructose or 99 HMF molecules (solute) were placed at the center of a 7 nm cubic box, with the solvation shell consisting of 330 (carboxymethyl)trimethylammonium cations, 87 acetone molecules, and 4200 water molecules; 330 Cl^- ions were added as counterions to neutralize the system, and the GROMOS 54A7 force field was employed for all simulations[1]. Total potential energy included valence terms

(bond stretching, angle bending, torsion) and nonbonded interactions, where nonbonded interactions were described by Lennard-Jones potentials with van der Waals interactions between distinct atom types calculated using standard geometric mean combination rules, long-range electrostatic interactions computed via the Particle Mesh Ewald method[2], a 1.2 nm cutoff for short-range van der Waals interactions, bond lengths constrained using the LINCS algorithm[3], and periodic boundary conditions applied in all directions. Each system underwent energy minimization of initial configurations using the steepest descent method, followed by a 400 ps NPT ensemble simulation for equilibration with a 1 fs time step where temperature was linearly annealed from 0 to 393 K; production runs were conducted for 50 ns under NPT conditions (393 K, 5.8 atm) with temperature regulated by the V-rescale thermostat and pressure maintained via the Parrinello-Rahman algorithm, trajectory analysis performed using GROMACS built-in tools, and visualization conducted with VMD 1.9.3 software.

Techno-economic analysis

Techno-economic analysis of HMF production from fructose was conducted in four sequential steps.

(1) Process modeling: A process flow diagram (Figure 6a) was developed, and corresponding models were constructed using Aspen Plus V12.0 (Aspen Technology) based on experimental data. The HMF production section achieves an 86.7% molar yield from fructose dehydration. For solvent recovery: post-reaction mixtures are cooled to 5 °C (chilled water), inducing crystallization of 90% BHC; acetone/water mixtures are recovered via throttle flashing and vacuum evaporation, liquefied with 244 K refrigerant, and recycled to the reactor. Excess water (by-product of dehydration) is removed in a fractionation tower post-acetone/water separation to maintain 30 wt% fructose in the feed. HMF purification involves acetone extraction (1:5 mass ratio) to separate HMF from residual BHC (10%) and unreacted fructose—insolubles are recycled to the reactor, while solubles undergo vacuum evaporation to recover acetone and yield 98.2 wt% pure HMF.

(2) Heat integration: Energy optimization was performed using Aspen Energy Analyzer V12.0. Post-integration, separation units dominated energy consumption: heating requirements for separation were 5.5× higher than for reaction, with cooling demands 29.6× greater. Process electricity consumption was estimated at 12 kW (Table S3, ESI†), with external sources supplying all heating, cooling, and electrical needs.

(3) Equipment sizing and cost analysis: Equipment sizing and cost estimation were conducted in Aspen Process Economic Analyzer V12.0, with all costs normalized to 2024. Capital and operating costs for all units are detailed in Table S4 (ESI†), using economic parameters listed in Table S2 (ESI†).

(4) Minimum selling price (MSP) calculation: Discounted cash flow analysis determined the MSP of HMF under defined financial assumptions (formula in ESI†). The MSP was iteratively adjusted until the project net present value reached zero at a 10% internal rate of return.

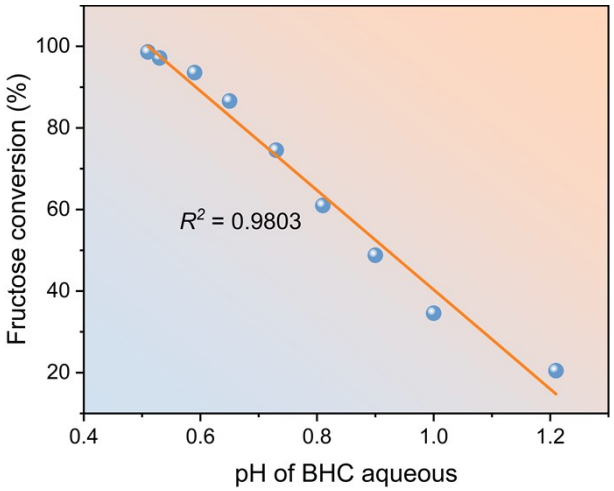

Fig. S1. Effect of the pH of BHC aqueous at different concentrations on the conversion of fructose.

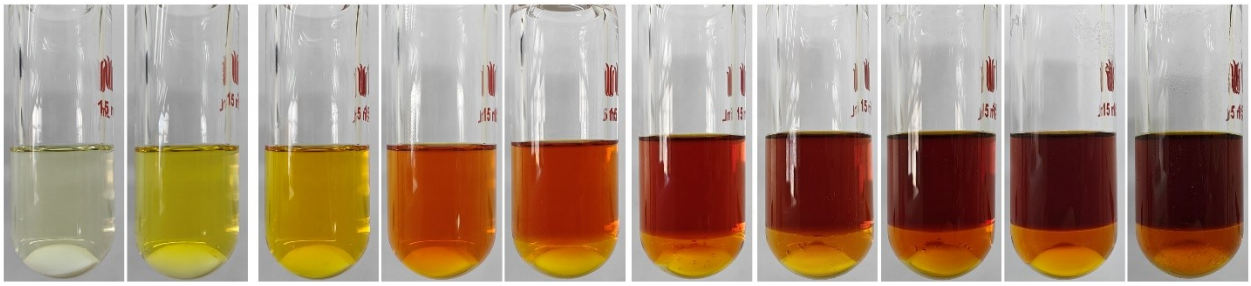

Fig. S2. Effect of BHC concentration on fructose dehydration.

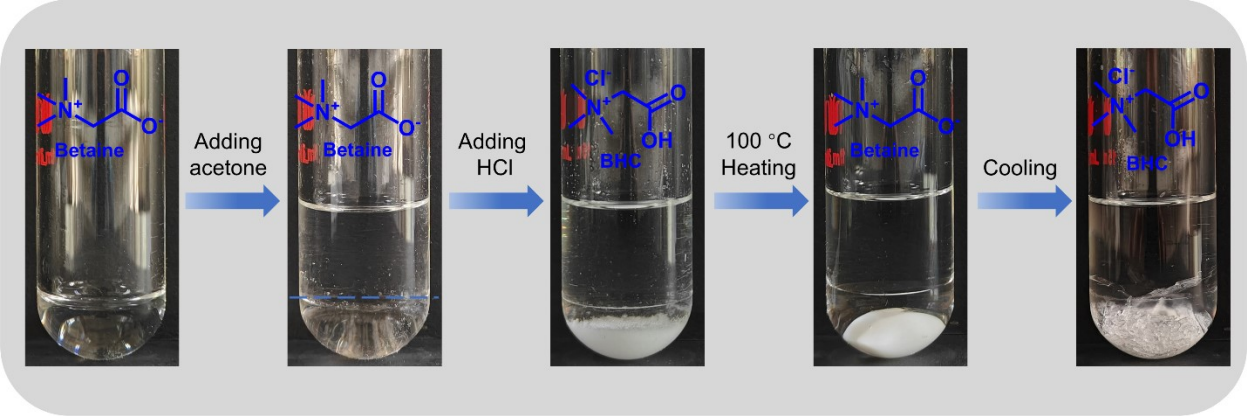

Fig. S3. Phase-switchable behavior of acetone/betaine aqueous solution system.

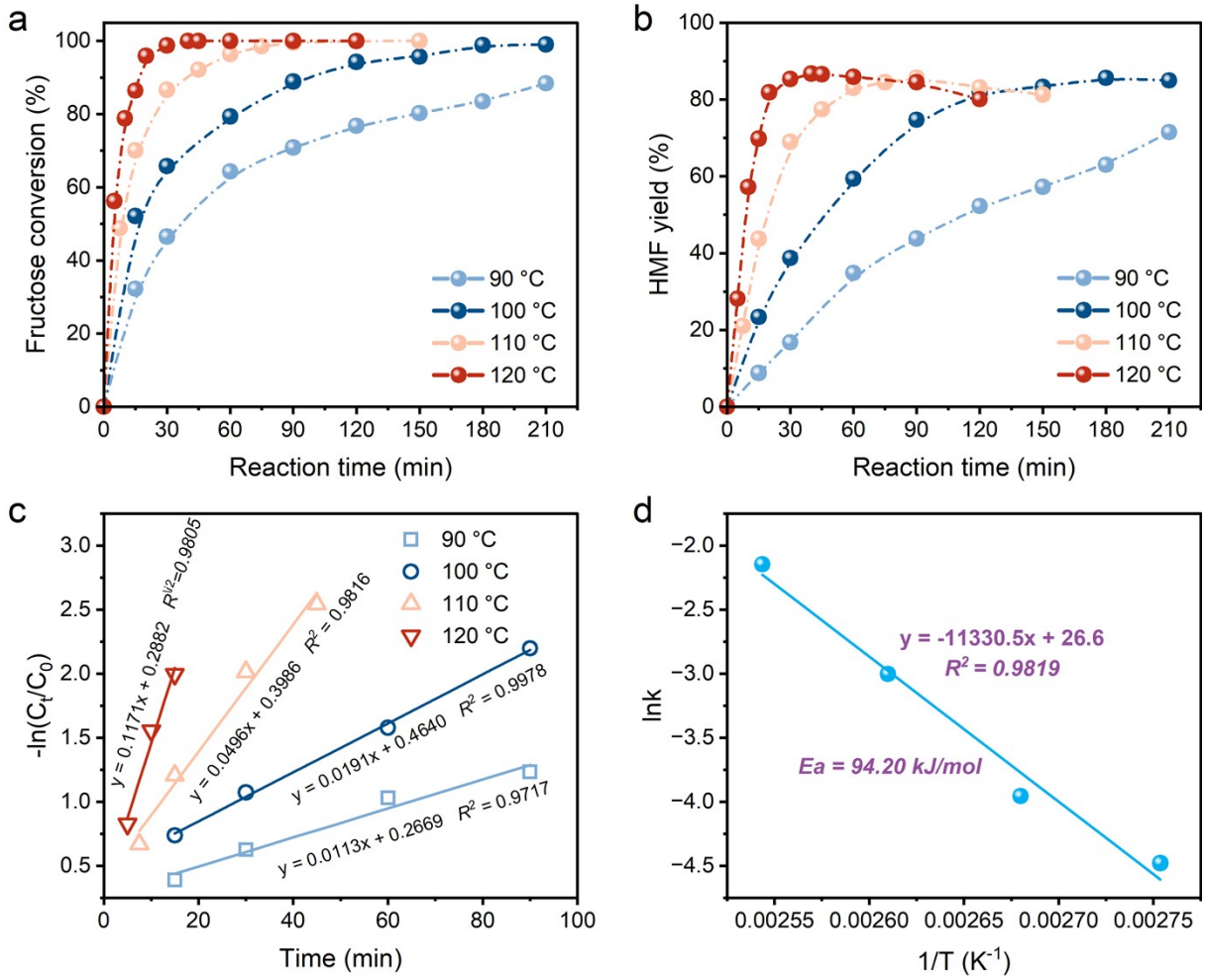

Fig. S4. (a, b) The effect of reaction temperature on fructose conversion and HMF yield. (c) Kinetic analysis for dehydration of fructose to HMF in the acetone/BHC aqueous solvent system. (d) Arrhenius plot of fructose dehydration in the acetone/BHC aqueous solvent system. Reaction conditions: 0.86 g of fructose, 2 mL of BHC aqueous, 8 mL of acetone.

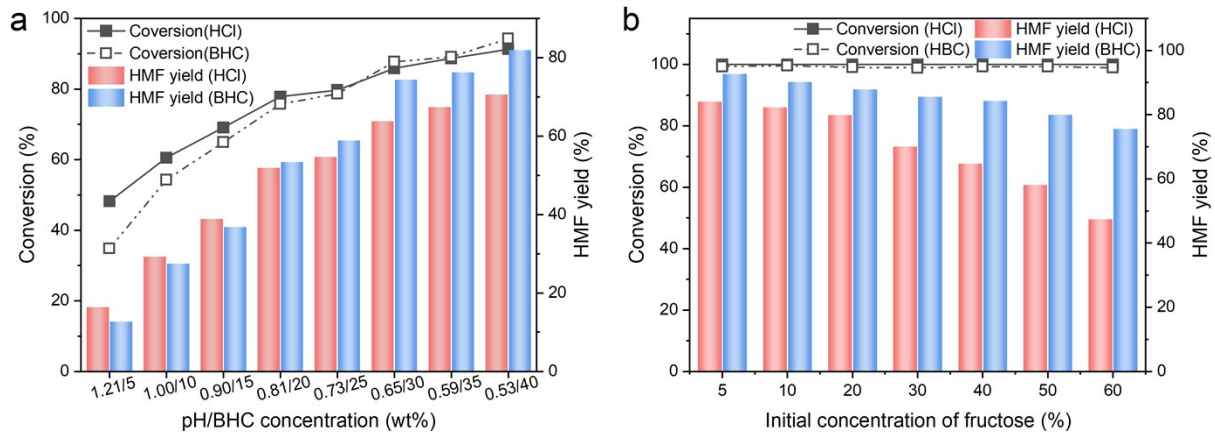

Fig. S5. (a) Effect of catalyst amount on fructose conversion and HMF yield in acetone-H_2O (HCl as catalyst) and acetone/ BHC aqueous systems. Reaction conditions: 2 mL of different pH HCl solution or different concentration BHC aqueous, 6 mL of acetone, 100 °C, 120 min. (b) Effect of fructose concentration on fructose conversion and HMF yield in acetone-H_2O and acetone/BHC aqueous systems. Reaction conditions: 2 mL pH = 0.53 HCl solution or 40 wt% BHC aqueous, 8 mL of acetone, 100 °C.

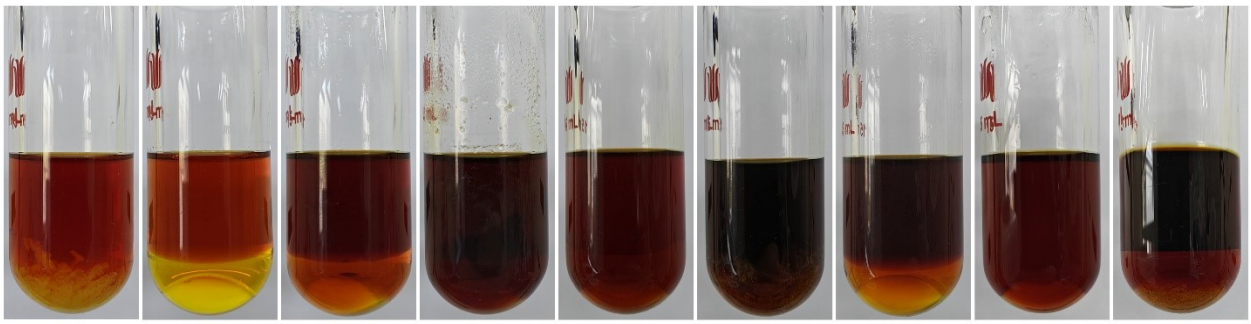

Fig. S6. The stratification status of the solvent systems after cooling at room temperature for 2 h.

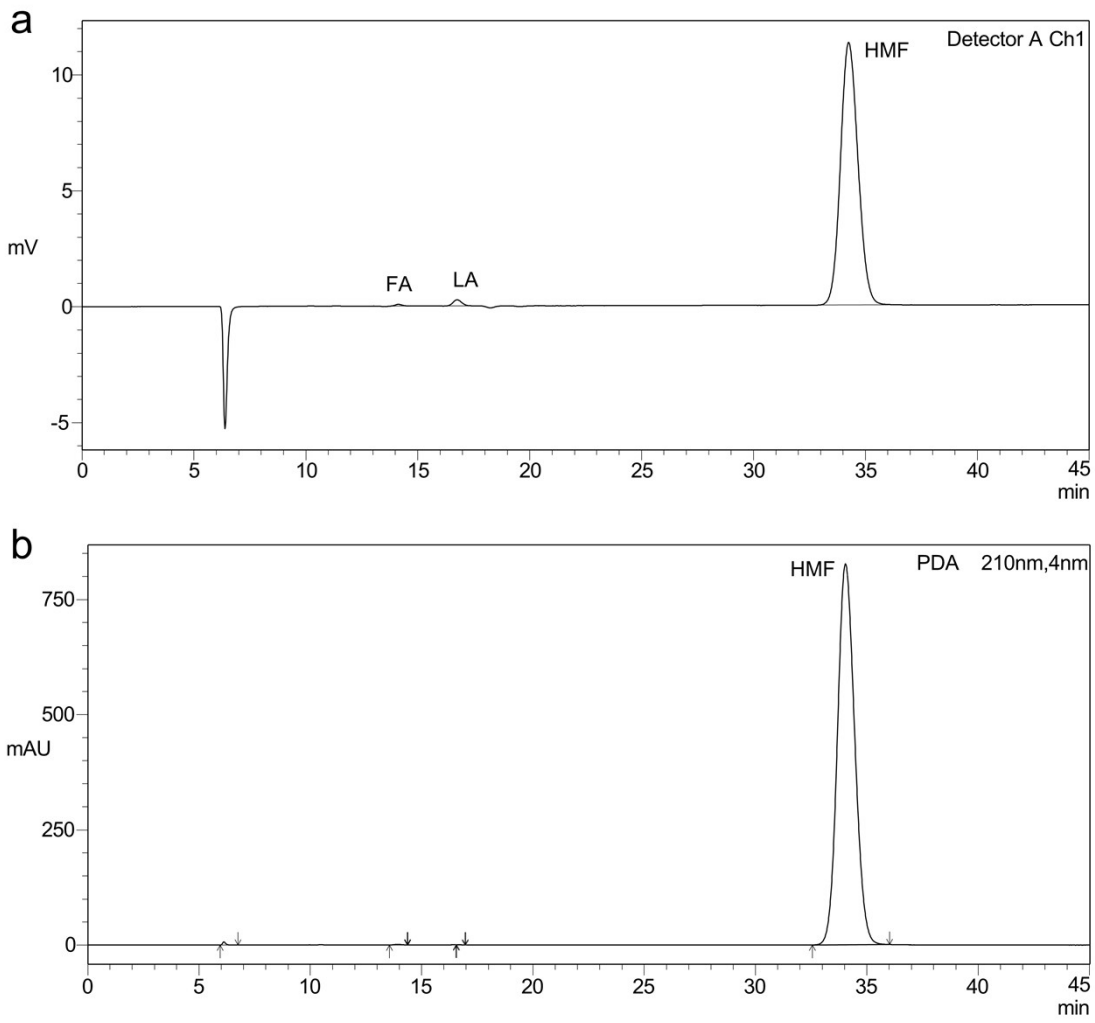

Fig. S7. HPLC chromatogram of products. (a) Chromatogram using refractive index detector, FA (14.1 min), LA (16.8 min), HMF (34.3 min). (b) Chromatogram using PDA detector, HMF (34.0 min).

Table S1. HMF yields and key reaction parameters of this study compared with literature studies that report on production of HMF from fructose and glucose in different reaction systems.

Substrate	Solvent system	Catalyst	Substrate concentration	Temp. /°C	Time /min	HMF yield/%	Ref.
Fructose	H_2O-DMSO-PVP/ MIBK-2-butanol	HCl	30 wt%	180	3	68.1	4
Fructose	TEAC/THF	$NaHSO_4 \cdot H_2O$	33.3 wt%	120	70	81.3	5
Glucose	TEAC/THF	$CrCl_3 \cdot 6H_2O$	33.3 wt%	120	70	51.4	5
Fructose	GVL/H_2O	H_2SO_4	3.2 wt%	130	10	73.0	6
Fructose	63 wt% $ZnCl_2$	HCl	2 wt%	120	/	53.3	7
Fructose	H_2O	NbPO	10 wt%	180	10	33.9	8
Fructose	$LiNO_3$-$NaNO_3$-KNO_3	/	2 wt%	135	30	37.0	9
Glucose	$LiNO_3$-$NaNO_3$-KNO_3	/	2 wt%	135	30	9.4	9
Fructose	[Bmim][OTf]	HCl	14 wt%	100	10	82.0	10
Fructose	1,4-Dioxane/H_2O	CTAB, H_2SO_4	50 wt%	140	15	58.6	11
Fructose	ChCl-BDO-PH	/	1 wt%	120	120	90.2	12
Fructose	ChCl/Acetonitrile	$H_4SiW_{12}O_{40}$	16.7 wt%	80	30	84.0	13
Fructose	DPhSO	/	33.3 wt%	140	660	68.4	14
Fructose	MIBK/H_2O-NaCl	[DBU-SO_3H][TsO]	4.5 wt%	120	60	85.0	15
Fructose	Acetone/H_2O	HCl	1 wt%	120	120	95.0	16
Fructose	Acetone/H_2O	HCl	5 wt%	120	20	85.0	16
Fructose	Acetone/H_2O	HCl	1.2 wt%	150	12	85.7	17
Glucose	Acetone/H_2O	HCl, $AlCl_3$	1.25 wt%	160	40	65.0	18
Fructose	Acetone/BHC	/	5 wt%	100	120	92.6	This work
Fructose	Acetone/BHC	/	30 wt%	120	40	86.7	This work
Fructose	Acetone/BHC	/	60 wt%	100	360	75.5	This work

Table S2. Aspen modules used for the corresponding units

No.	Unit number	Aspen Module
1	R-1	RStoic
2	S-1, A-1	Sep
3	H-1, H-2	HeatX
4	C-1, C-2, C-3, C-4	Heat
5	P-1, P-2	Pump

Table S3. Energy requirements for the HMF production (with heat integration).

Unite	Energy required				
Fructose to HMF	Heating, kW	Electricity, kW	Refrigerating, kW	Cooling by Circulated water supply, kW	Cooling by Chilled water, kW
Reaction unit	1585	6	0	-152	0
Separation Unit	8640	6	-460	-1100	-2939
Total	10225	12	-460	-1252	-2939

Table S4. The project investment and operating costs. (10^6\$/a or 10^6\$)

	Fructose feedstock
Process section	
Total Capital Cost	8.38
OSBL[a]	3.35
Total project investment [b]	11.74
Raw material	
Feedstock	11.13
Catalyst	~0
Acetone solvent makeup	0.13
Refrigeration, -29 °C－28 °C	0.02
Steam saturated, 124℃	8×10^{-3}
Cooling water, 32 °C－43 °C	0.04
Chilled water, 5 °C－15 °C	0.38
Electricity	0.06
Wastewater disposal	0.32
Total variable operating costs	12.08
HMF production & Specifications	
Production (tonne/yr)	10000
Purity (wt%) & recovery (%)	98.2 & >97.6

[a] OSBL (outside battery limits of the plant) includes infrastructure costs for waste disposal, on-site storage, and utilities.

[b] the total project investment including the total installed cost.

The minimum selling price of HMF is obtained as follows[19, 20]:

HMF sales = Total variable operating costs + Total project investment/20 + Average income tax + Average ROI

HMF sales (\$/tonne HMF) = 12080000/10000 + 11740000/10000/20 + (1208 + 59) × 0.21 / (1 - 0.21) + (1208 + 59 + 337) × 0.10

= 1208 + 59 + 337 + 160

= 1764

Table S5. List of economic parameters and assumptions for the HMF production (with heat integration).

Fructose price ($/tonne)	675 [a]
Acetone price ($/tonne)	810.44 [b]
HMF price ($/tonne)	8570 [a]
Wastewater treatment cost ($/tonne)	0.570 [c]
Low pressure steam cost ($/tonne)	7.426 [e]
Refrigerant, -29 °C—28 °C ($/tonne)	1.433[e]
Electricity price ($/kWh)	0.0572 [c]
Cooling water, 32 °C—43 °C ($/tonne)	1.086×10^{-2} [e]
Chilled water, 5 °C—15 °C ($/GJ)	4.43[f]
Operating mode	Continuous
Plant life (years)	20 [d]
Plant operating hours per year (hours)	8000 [d]
Discount rate (%)	10 [d]
General plant recovery period (years)	7 [d]
Corporate income rate (%)	21 [d]
Equity financing (%)	40 [d]
Loan terms	10-years loan at 8% APR [d]
Working capital	5% of fixed capital investment [d]
Length of start-up period (weeks)	1 [d]
Revenues during start-up (%)	50 [d]
Fixed costs during start-up (%)	100 [d]

[a] The price standards used refer to China's chemical market price level in 2024
[b] Taken from refence prices by *P. Desir et al.* [21]
[c] Taken from refence prices by *A. H. Motagamwala et al.*[16]
[d] Data were taken from a study by NREL[22]
[e] Estimated from the refence by *A. H. Motagamwala et al.* [16]
[f] Estimated from the refence by *W. L. Luyben.* [23]

References and Notes

1. N. Schmid, A. P. Eichenberger, A. Choutko, S. Riniker, M. Winger, A. E. Mark and W. F. van Gunsteren, *European Biophysics Journal*, 2011, **40**, 843-856.
2. T. Darden, D. York and L. Pedersen, *The Journal of Chemical Physics*, 1993, **98**, 10089-10092.
3. B. Hess, H. Bekker, H. J. C. Berendsen and J. G. E. M. Fraaije, *Journal of Computational Chemistry*, 1997, **18**, 1463-1472.
4. Y. Román-Leshkov, J. N. Chheda and J. A. Dumesic, *Science*, 2006, **312**, 1933-1937.
5. Q. Cao, X. Guo, J. Guan, X. Mu and D. Zhang, *Applied Catalysis A: General*, 2011, **403**, 98-103.
6. L. Qi, Y. F. Mui, S. W. Lo, M. Y. Lui, G. R. Akien and I. T. Horváth, *ACS Catalysis*, 2014, **4**, 1470-1477.
7. T. Deng, X. Cui, Y. Qi, Y. Wang, X. Hou and Y. Zhu, *Chemical Communications*, 2012, **48**, 5494-5496.
8. C. Antonetti, M. Melloni, D. Licursi, S. Fulignati, E. Ribechini, S. Rivas, J. C. Parajó, F. Cavani and A. M. Raspolli Galletti, *Applied Catalysis B: Environmental*, 2017, **206**, 364-377.
9. P. Bhaumik, H.-J. Chou, L.-C. Lee and P.-W. Chung, *ACS Sustainable Chemistry & Engineering*, 2018, **6**, 5712-5717.
10. A. A. Ghatta, J. D. E. T. Wilton-Ely and J. P. Hallett, *ChemSusChem*, 2019, **12**, 4452-4460.
11. Y. Hu, H. Li, P. Hu, L. Li, D. Wu, Z. Xue, C. Hu and L. Zhu, *Green Chemistry*, 2023, **25**, 661-670.
12. M. Li, P. Zhang, S. Hu, D. Min, J. Tang, Y. Zhang and L. Jiang, *Fuel*, 2025, **389**, 134548.
13. N. Thanheuser, J. T. Groteguth, W. Leitner, J. Esteban and A. J. Vorholt, *ChemSusChem*, 2025, **18**, e202401485.
14. T. Zhang, Y. Hu, L. Huai, Z. Gao and J. Zhang, *Green Chemistry*, 2021, **23**, 3241-3245.
15. T. H. Nguyen, D. Q. Mai, D. A. L. Nguyen, M. N. T. Le and P. H. Tran, *Energy & Fuels*, 2025, **39**, 22235-22247.
16. A. H. Motagamwala, K. Huang, C. T. Maravelias and J. A. Dumesic, *Energy & Environmental Science*, 2019, **12**, 2212-2222.
17. H. Zhu, X. Guo, Y. Si, Q. Du, Y. Cheng, L. Wang and X. Li, *Chemical Engineering Science*, 2023, **267**, 118352.
18. H. Zhu, Y. Zhang, X. Guo, Y. Cheng, L. Wang and X. Li, *Industrial & Engineering Chemistry Research*, 2022, **61**, 5661-5671.
19. A. I. Torres, P. Daoutidis and M. Tsapatsis, *Energy & Environmental Science*, 2010, **3**, 1560-1572.
20. A. I. Torres, M. Tsapatsis and P. Daoutidis, *Computers & Chemical Engineering*, 2012, **42**, 130-137.
21. P. Desir, B. Saha and D. G. Vlachos, *Energy & Environmental Science*, 2019, **12**, 2463-2475.
22. R. Davis, L. Tao, E. Tan, M. Biddy, G. Beckham, C. Scarlata, J. Jacobson, K. Cafferty, J. Ross and J. Lukas, *Process design and economics for the conversion of lignocellulosic biomass to hydrocarbons: dilute-acid and enzymatic deconstruction of biomass to sugars*

and biological conversion of sugars to hydrocarbons, National Renewable Energy Lab.(NREL), Golden, CO (United States), 2013.
23. W. L. Luyben, *Principles and case studies of simultaneous design*, John Wiley & Sons, 2012.